

Mechanical Ringdown Studies of Large-Area Substrate-Transferred GaAs/AlGaAs Crystalline Coatings

Steven D. Penn^{1,*}, Maya M. Kinley-Hanlon², Ian A. O. MacMillan^{2,3}, Paula Heu⁴, David Follman⁴, Christoph Deutsch⁵, Garrett D. Cole^{4,5}, and Gregory M. Harry²

¹*Department of Physics, Hobart and William Smith Colleges, 300 Pulteney Street, Geneva, NY 14456, USA*

²*Department of Physics, American University, 4400 Massachusetts Avenue, Washington, DC 20016, USA*

³*Department of Physics, Georgetown University, 3700 O Street NW, Washington, DC 20057, USA*

⁴*Crystalline Mirror Solutions LLC, 114 East Haley Street Suite G, Santa Barbara, CA 93101, USA*

⁵*Crystalline Mirror Solutions GmbH, Lehargasse 1, A-1060 Vienna, Austria*

*Corresponding author: penn@hws.edu

November 16, 2018

Abstract

We investigated elastic loss in GaAs/AlGaAs multilayers to help determine the suitability of these coatings for future gravitational wave detectors. We measured large (≈ 70 -mm diameter) substrate-transferred crystalline coating samples with an improved substrate polish and bonding method. The elastic loss, when decomposed into bulk and shear contributions, was shown to arise entirely from the bulk loss, $\phi_{\text{Bulk}} = (5.33 \pm 0.03) \times 10^{-4}$, with $\phi_{\text{Shear}} = (0.0 \pm 5.2) \times 10^{-7}$. These results predict the coating loss of an 8-mm diameter coating in a 35-mm long cavity with a 250- μm spot size (radius) to be $\phi_{\text{coating}} = (4.78 \pm 0.05) \times 10^{-5}$, in agreement with the published result from direct thermal noise measurement of $\phi_{\text{coating}} = (4 \pm 4) \times 10^{-5}$. Bonding defects were shown to have little impact on the overall elastic loss.

1 Introduction

The direct measurement of gravitational waves [1, 3], as predicted by Einstein's General Theory of Relativity, has opened a new window on the universe and launched the field of multi-messenger astronomy [4, 9, 20]. Interferometric gravitational wave detectors, such as LIGO [2], Virgo [8], and KAGRA [10] are precision optical instruments designed specifically to detect these distortions in space-time. Thermally-driven fluctuations of the optical coatings of the detector test mass mirrors are a significant limitation to their sensitivity [2] and astronomical reach. Reducing coating thermal noise to near or below the standard quantum limit [27, 25, 35] is a key goal for future detectors [5]. Thermal noise is expected to limit the sensitivity of

the current LIGO and Virgo detectors [2, 8] in the mid-frequency band, 50-150 Hz, which is their region of highest sensitivity [2]. In addition, thermal noise will present a significant challenge when designing future, more sensitive, gravitational wave detectors [6]. Ultimately, the minimization of thermal noise will allow for fully quantum-limited interferometry.

crystalline coatings have shown promising results, with sub-ppm absorption and scatter in-line with that seen in ion-beam sputtered coatings [30] currently employed in gravitational wave detectors [2]. These promising optical properties now motivate us to explore the thermal noise performance of large-area crystalline coatings.

Epitaxial GaAs/Al_{0.92}Ga_{0.08}As (AlGaAs) multilayers have demonstrated low elastic losses

in free-standing microresonator experiments at both room and cryogenic temperatures [16, 15]. Moreover, direct thermal noise measurements in reference-cavity-stabilized laser systems have confirmed the low loss of these single crystal films $\phi_{\text{coating}} = (4 \pm 4) \times 10^{-5}$ once transferred to a final optical substrate and implemented as a high-reflectivity interference coating [18]. In addition to their low elastic loss, recent optical characterization efforts on large-area (50-mm diameter) crystalline coatings have shown promising results, with sub-ppm absorption and scatter in-line with that seen in ion-beam sputtered coatings [30] as currently employed in gravitational wave detectors. In terms of size scaling, crystalline coatings may currently be manufactured with diameters up to 20 cm using commercially available wafers, with the possibility for realizing 40-cm diameter optics using custom-fabricated GaAs substrates. While these results are promising for future implementation in gravitational wave detectors, noise in these coatings have thus far been probed on either small-area optics (typical coating diameters from 5-8 mm) or with small spot sizes at the millimeter scale. In contrast, current LIGO test mass mirrors have 34-cm diameter faces [12] with cm-scale optical spots, and future gravitational wave interferometers may employ larger mirrors in part as a method to reduce coating thermal noise which depends inversely on the beam diameter.

Large beams require a uniform coating surface across the full face of the suspended optic. Any defects, even far from the beams center, could generate excess optical loss, thereby increasing shot noise and possibly increasing mechanical loss in the coating, reducing the detector sensitivity. On the later point, in the course of developing larger AlGaAs mirror coatings, concerns have been raised that low elastic losses may be difficult to achieve at larger size scales. Variations in the dissipation mechanism due to imperfections or varying bond strength across a sample may allow for low losses to be achieved in small scale measurements, but not for increased sample sizes. For larger samples, the increased coating area also increases the likelihood of a

bond defect occurring between the AlGaAs coating and the substrate. These defects could be expected to increase the elastic loss.

We report here on elastic loss measurements on a set of two 70.1-mm diameter AlGaAs crystalline coatings (Samples 2 & 4), with almost a factor of 80 larger coating area than previously investigated. In order to minimize potential interface losses the silica substrates were precision polished and efforts were made to optimize the GaAs-to-silica bond quality. After production, both samples exhibited about 10 visible defects and a few larger flaws along the edge. The elastic loss was measured for both samples using mechanical ringdown.

Following the initial loss measurement, Sample 4 was subjected to a selective chemical etching process to remove the bonding defects and was remeasured. The coating elastic loss was then calculated for the three sets of measurements (Samples 2, 4, & 4 etched). We found that the coating loss before and after etching showed only minor differences, indicating that the bond defects did not contribute significantly to the loss. In addition, the coating elastic loss measured for Mode 1 was less than that measured in any previous experiments with AlGaAs, indicating no significant excess loss induced by interfacial defects. Finally the separate components of elastic loss extracted from these measurements predict a coating loss for a 35-mm optical reference cavity that is consistent with published values [18].

2 Background

Brownian thermal noise can be described by the Fluctuation-Dissipation Theorem [13, 21], which demonstrates that the fluctuations in the state of a system and the system's dissipation can both be described by an elastic loss angle, the ratio of the imaginary part of the complex elastic constant to the real part. In 1998, Levin used the Fluctuation-Dissipation Theorem to calculate the contribution of thermal noise in the test mass mirror coatings to LIGO's overall sensitivity [29]. This calculation was a revelation to the

gravitational wave community, revealing that the thermal noise contribution from a few micrometers of lossy coating material could greatly exceed the thermal noise from the > 10 cm thick fused silica substrate. When Levin's derivation is applied to the case of amorphous mirror coatings on gravitational wave detector test masses, the coating thermal noise equation is given by [24]:

$$S_X(f) = 2k_B T \phi_{\text{eff}} \frac{1 - \sigma^2}{\pi^{3/2} f w Y}, \quad (1)$$

where S_x is the power spectral density of position fluctuations, f is the frequency, k_B is the Boltzmann constant, T is the temperature, σ is the Poisson ratio of the optic substrate material, w is the half-width of the Gaussian mode of the laser, Y is the Young's modulus of the optic substrate, and

$$\phi_{\text{eff}} = \phi + \phi_{\text{coating}} \frac{2d - 4d\sigma}{\sqrt{\pi} w (1 - \sigma)}, \quad (2)$$

where ϕ is the loss angle of the optic substrate, d is the thickness of the coating, and ϕ_{coating} is the loss angle of the coating. Equation 2 is a simplification of the full formula for ϕ_{eff} assuming only a single loss angle ϕ_{coating} and elastic constant Y can be used to characterize the elasticity of the coating material.

For our experiments, the samples consist of thin coating layers bonded to or deposited on thin substrates formed from a very low loss material, typically fused silica. The elastic loss of the sample may be determined by measuring the modal Q factor via mechanical ringdown. This weakly-damped system can be driven to resonance and then allowed to freely ringdown with the amplitude describing a decaying exponential $A_0 e^{-t/\tau}$. The quality factor and elastic loss are related by $Q = \pi f_0 \tau = 1/\phi_{\text{sample}}$ where f_0 is the resonant frequency of the normal mode.

The elastic loss angle is the fraction of energy dissipated during each oscillation. Therefore, one can extract the coating loss using

$$\phi_{\text{coating}} = \frac{\phi_{\text{sample}} - R_{\text{substrate}} \phi_{\text{substrate}}}{R_{\text{coating}}}, \quad (3)$$

where $R_{\text{substrate}} = E_{\text{substrate}}/E_{\text{sample}} \approx 1$ and $R_{\text{coating}} = E_{\text{coating}}/E_{\text{sample}}$ are the energy ratios of the system components, also known as

the dissipation dilution factors. The energy ratios, which were calculated using a finite element model, are provided in Table 2.

AlGaAs, which is a face-centered cubic crystal, has an equation of elasticity that is expressed, using Voight notation, as $\sigma_I = c_{IJ} \epsilon_J$, where the elasticity matrix, c_{IJ} depends on three independent constants.

$$c_{IJ} = \begin{bmatrix} c_{11} & c_{12} & c_{12} & & & \\ c_{12} & c_{11} & c_{12} & & & \\ c_{12} & c_{12} & c_{11} & & & \\ & & & c_{44} & & \\ & & & & c_{44} & \\ & & & & & c_{44} \end{bmatrix} \quad (4)$$

In Eqn. 4 the unspecified elements are zero. For AlGaAs, $c_{11} = 119.94$ GPa, $c_{12} = 55.38$ GPa, and $c_{44} = 59.15$ GPa. For each of the three elastic constants, there should be a unique loss angle, ϕ_{11} , ϕ_{12} , and ϕ_{44} . The coating loss angle is then given by:

$$\phi_{\text{coating}} = R_{11} \phi_{11} + R_{12} \phi_{12} + R_{44} \phi_{44}, \quad (5)$$

where $R_{xx} = E_{xx}/E_{\text{coating}}$ and E_{xx} is the elastic energy in the xx deformation. (11 = parallel stress-strain, 12 = orthogonal stress-strain, and 44 = shear stress-strain). Because a single loss angle is measured for each mode of the sample, one determines the contributing loss angles by fitting the sample loss as a function of mode frequency. This method requires that the energy ratio functions be linearly independent in order to avoid degeneracy.

Unfortunately R_{11} and R_{12} are similar functions of mode, which makes it difficult to distinguish ϕ_{11} and ϕ_{12} . It should be possible to separate these loss angles by examining modes with quadrupole symmetry and comparing the loss of degenerate states that are aligned and unaligned with the crystal axes. However, for the modes we measured this was not possible and as can be seen in Figure 1, R_{11} and R_{12} have a linear dependence.

Therefore, for the remainder of this paper we will characterize the elastic loss in AlGaAs coatings using a bulk/shear decomposition, a method usually employed in analyzing the loss

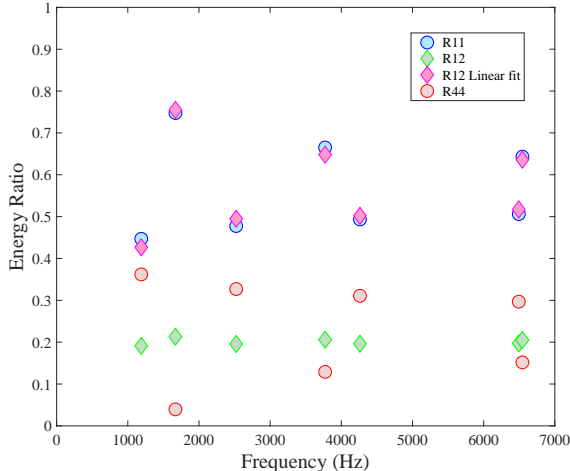


Figure 1: The energy ratios, R_{11} , R_{12} , and R_{44} , for the modes measured in Sample 4. The R_{12} Linear Fit demonstrates the R_{11} , R_{12} dependence since $R_{11} \approx m \cdot R_{12} + b$

and thermal noise in amorphous coatings [26, 7]. Bulk/Shear decomposition is an appropriate choice in this case because $R_{\text{shear}} = R_{44}$ and R_{bulk} is composed from R_{11} and R_{12} . As will be shown in the Results Section 4, this choice appears to reflect a natural separation for AlGaAs coatings (see Figure 7).

The high reflectivity coatings used currently in Advanced LIGO and Advanced Virgo are multilayers of amorphous metal oxides, with alternating layers of SiO_2 (low index) and TiO_2 -alloyed Ta_2O_5 (high index) deposited by ion-beam sputtering [22, 23, 19, 31, 32]. These dielectric multilayer coatings exhibit excellent optical properties including <1 ppm of absorption and ppm-level scatter [12] and can be applied over a large area on a variety of optical substrates. However, the main drawback of these coatings is the high elastic loss of the high index material, which generates unacceptably high levels of coating thermal noise. The Initial LIGO coatings were a $\text{SiO}_2 / \text{Ta}_2\text{O}_5$ quarter-wave multilayer coating with an elastic loss of $\approx 3 \times 10^{-4}$ [31]. For Advanced LIGO the coatings were improved by alloying the Ta_2O_5 layers with TiO_2 , which reduced the coating loss to $\approx 2 \times 10^{-4}$ [22].

Significant improvements in performance are still being investigated for low-noise and high-

reflectivity coatings. Specifically, for the recently funded “A+” upgrade for Advanced LIGO, the goal is to reduce the coating elastic loss by another factor of 2–4 [11].

Single-crystal interference coatings, such as GaAs/AlGaAs, are an attractive candidate for future gravitational wave detectors. This material simultaneously exhibits excellent optical quality [17, 30] and low elastic loss [16, 15], with a measured coating loss of $\phi_{\text{coating}} = (4 \pm 4) \times 10^{-5}$ at room temperature when implemented in an optical reference cavity [18]. These coatings consists of alternating lattice-matched single crystal films deposited via an epitaxial growth process. $\text{Al}_x\text{Ga}_{1-x}\text{As}$, $0 < x < 1$, is a ternary alloy of GaAs and AlAs III-V compound semiconductors, both consisting of a face-centered cubic unit cell and a nearly matching lattice constant across all Al compositions. The ability to generate low-strain heterostructures with reasonable refractive index contrast allows for the generation of high-performance single-crystal optical interference coatings as initially demonstrated by van der Ziel and Illegems [34]. One major engineering challenge to this material system, being a single-crystal structure, is the need for lattice matching in epitaxy, which precludes the growth of such heterostructures on arbitrary optical surfaces, including direct-deposition on amorphous or mismatched crystalline structures. To overcome this limitation, epitaxial multilayers are removed from their initial growth wafers and directly bonded to the final optical surface. With this approach, high purity and low defect density single crystal materials can be combined with arbitrary (including curved) optical substrates [17].

3 Method

The 3” diameter fused silica substrates (Corning 7980) employed in our experiment were obtained from a commercial wafer manufacturer with specifications of <0.5 -nm RMS microroughness, a wafer bow/warp of $<15 \mu\text{m}$, and 1-mm thickness with a total thickness variation of $<10 \mu\text{m}$. Before measurement (and coating), Sample

Mode	Initial Sample			Etched Sample		
	R_{coating}	R_{bulk}	R_{shear}	R_{coating}	R_{bulk}	R_{shear}
1	0.0218	0.0347	0.965	0.0242	0.0381	0.962
2	0.0228	0.320	0.680	0.0216	0.315	0.685
3	0.0193	0.0568	0.943	0.0166	0.0584	0.942
4	0.0233	0.239	0.761	0.0219	0.251	0.749
5	0.0175	0.0724	0.928	0.0149	0.0698	0.930
6	0.0161	0.0839	0.916	0.0133	0.0827	0.917
7	0.0226	0.217	0.783	0.0189	0.243	0.758

Table 1: Dissipation dilution factors, R , used to extract the coating loss and the bulk/shear components of the coating loss.

4 was annealed at a maximum temperature of 950 C for approximately 6 hours in a clean air atmosphere. Sample 2 was not annealed. Each sample was then suspended in a vacuum bell jar from a welded silica fiber suspension [24]. A vacuum was maintained below 10^{-5} Torr throughout the measurement. This technique for measuring mechanical Q s has been described in several papers [28, 24, 22, 31, 19, 32]. We summarize the process in the text below and include a diagram of the experiment in Figure 2.

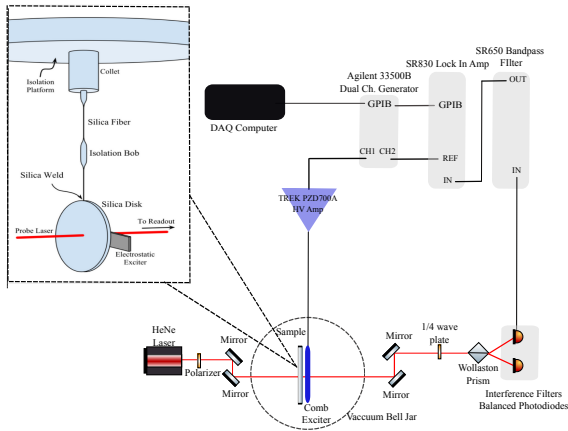


Figure 2: Experimental setup used to measure the elastic loss. The inset shows how the sample is hung with a thin silica fiber, connected with an isolation bob for vibration isolation. The comb capacitor, in blue, is situated close to the sample for efficient driving.

To excite the mechanical modes of the sample, a comb capacitor (exciter) was placed near the suspended sample (see the inset in Figure 2).

The exciter generates an alternating gradient electric field that exerts an oscillatory force on the induced dipole ($\vec{F} = \vec{p} \cdot \nabla \vec{E}$). The sample is driven at the normal mode frequency. Excitation is ceased and the free decay is measured by recording the strain-induced birefringence (ellipsometry) [24]. The data is heterodyned using a lock-in amplifier and recorded using a LabView data acquisition code written by the author (SP). A typical data run is recorded over a period of at least twice the exponential decay factor or the time it takes the amplitude to decrease by a factor of e^{-2} . Several data runs are recorded for each mode, and the loss for each mode is the average of the results weighted by the fit uncertainty assuming Gaussian statistics. The loss was measured for the bare substrate and for the coated samples. The coating loss was calculated using Equation 3.

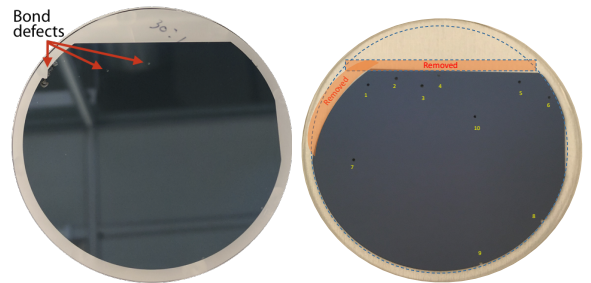


Figure 3: Photographs of the Sample 4 before (left) and after (right) the selective defect removal process. The etched regions have been highlighted in the right panel.

After the measurement of the substrates, the

samples were coated with a high-reflectivity Al-GaAs multilayer with 35.5 layers of alternating GaAs (76.43 nm) and $\text{Al}_{0.92}\text{Ga}_{0.08}\text{As}$ (89.35 nm), for a target optical transmission of 10 ppm at 1064 nm. Similar to previous crystalline coating efforts [18, 33, 14, 15, 30], we begin by growing a single-crystal multilayer by molecular beam epitaxy (MBE) on a 150-mm diameter GaAs wafer (in a 7" \times 6" wafer configuration). For this effort, we deposit 36 layer pairs of quarter-wave (optical thickness at a wavelength of 1064 nm) GaAs/ $\text{Al}_{0.92}\text{Ga}_{0.08}\text{As}$ with the final Al-containing layer acting as an etch stop for selective substrate removal. Following the MBE growth process, each 6" wafer is lithographically patterned to generate two approximately 3" diameter coating discs with a large "flat" for crystal orientation identification as well as to pull back the coating from the heat-affected zone generated in fiber welding. These discs were inspected, thoroughly cleaned, and then directly bonded to a 3" diameter, 1-mm thick precision polished fused silica substrate. Following the substrate-transfer coating process, the mirror surface was again thoroughly cleaned and inspected for imperfections. Then the sample's Q were remeasured at the same normal modes. Similar to the coating investigated in [30], completed samples exhibited a small population of visible defects. The example shown in Figure 3 had imperfections at 12 locations, including point defects $>50 \mu\text{m}$ in diameter, as well as larger, unbonded regions at the coating edge.

Following the measurements on the coated samples, Sample 4 was further processed to eliminate the macroscopic bond defects. First the mirror surface was covered with photoresist. Then, a filtered (short-wavelength blocking) white-light optical microscope was used to identify and expose, via removal of said filter, the applied photosensitive polymer film over each defect. After exposure, the mirror was submerged in a developer solution to remove the photoresist at the defect sites, and a selective phosphoric-acid based wet chemical etch ($\text{H}_3\text{PO}_4:\text{H}_2\text{O}_2:\text{H}_2\text{O}$ 1:5:15) was used to remove the undesired coating material. Our experience has shown that this etch has high selectivity with SiO_2 and we

Mode	Freq. (kHz)	Loss Angle ($\times 10^{-5}$)		
		ϕ_{sample}	$\phi_{\text{substrate}}$	ϕ_{coating}
1	1.074	0.0955	0.0657	1.4400
3	2.462	0.1889	0.1131	4.0500
4	3.778	0.3351	0.0172	13.6400
6	6.510	0.2398	0.1680	4.6300
7	6.566	0.3090	0.0227	12.6900

Table 2: Sample 2: Elastic loss of initial coating with bond defects.

Mode	Freq. (kHz)	Loss Angle ($\times 10^{-5}$)		
		ϕ_{sample}	$\phi_{\text{substrate}}$	ϕ_{coating}
1	1.077	0.0404	0.0069	1.5500
2	1.624	0.3734	0.0135	15.8000
3	2.473	0.0970	0.0391	3.0500
4	3.792	0.3122	0.0063	13.1100
6	6.536	0.1028	0.0664	2.3300

Table 3: Sample 4: Elastic loss of initial coating with bond defects.

can recover a pristine surface with sub-Angstrom RMS microroughness. When the etching process was complete, the loss in Sample 4 was measured again.

4 Results

Mode	Freq. (kHz)	Loss Angle ($\times 10^{-5}$)		
		ϕ_{sample}	$\phi_{\text{substrate}}$	ϕ_{coating}
1	1.071	0.0646	0.0069	2.3900
2	1.624	0.3689	0.0135	16.4700
3	2.472	0.0927	0.0391	3.2800
4	3.792	0.2947	0.0063	13.1800
6	6.530	0.1130	0.0664	3.5800
7	6.596	0.2554	0.0062	13.2200

Table 4: Sample 4: Elastic loss of etched coating with bond defects removed.

The elastic loss of coated samples and the bare substrates are listed in Tables 2 & 3 for the initial samples (before etching). The elastic loss of the coating is calculated using Equation 3 and

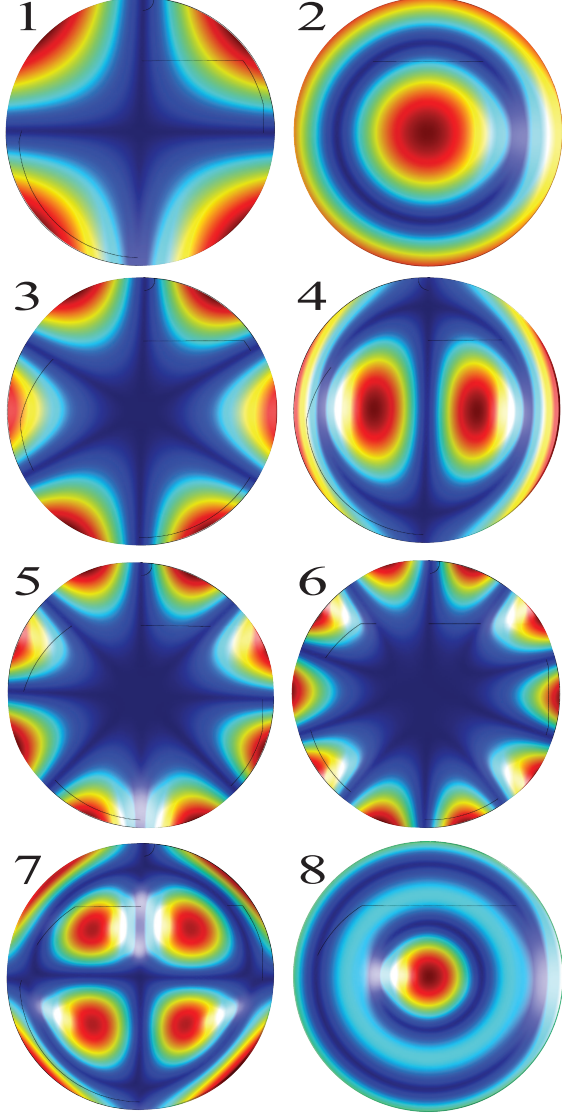


Figure 4: Modes 1–8 of the coating sample. The *radial* modes (1, 3, 5, 6) are dominated by shear energy. The *drumhead* modes (2, 4, 7, 8) have 1/3 of their energy in bulk stress. Modes 5 and 8 are presented for completeness, but no data was collected on these modes.

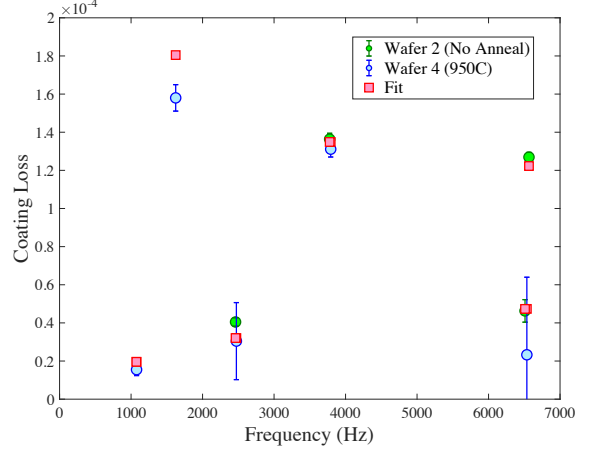


Figure 5: Coating loss of the initial samples with bond defects. A fit of bulk and shear losses yielded $\phi_{\text{Bulk}} = (5.64 \pm 0.10) \times 10^{-4}$ and $\phi_{\text{Shear}} = (0.0 \pm 1.5) \times 10^{-6}$.

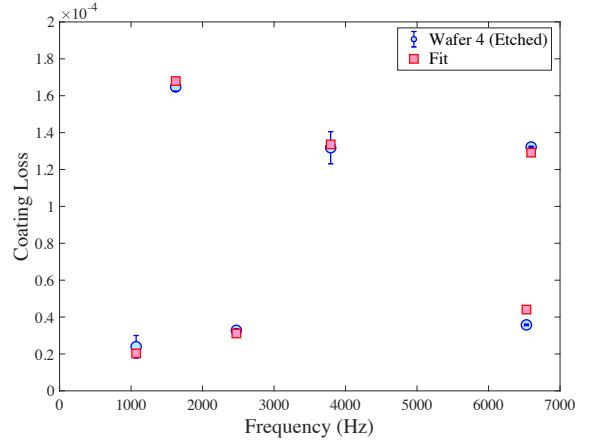


Figure 6: Coating loss ϕ_{coat} for Sample 4 with the bond defects selectively etched away. A fit of bulk and shear losses yielded $\phi_{\text{Bulk}} = (5.33 \pm 0.03) \times 10^{-4}$ and $\phi_{\text{Shear}} = (0.0 \pm 5.2) \times 10^{-7}$.

the R values from Table 2. Figure 5 shows the coating loss for the initial samples as a function of modal frequency. The loss was sharply divided with the loss in the drumhead modes (2,4,7) being about $4\times$ higher than the loss in the radial modes (1,3,6). This pattern of loss bifurcation, which has been observed previously in amorphous coatings [7] (except in that case the radial modes had higher loss), indicated a large difference in the loss from bulk and shear motion. From this observation, we chose to ana-

lyze the AlGaAs samples with a bulk and shear decomposition.

We decomposed the coating loss into bulk and shear losses using the equation

$$\phi_{\text{coating}} = R_{\text{bulk}}\phi_{\text{bulk}} + R_{\text{shear}}\phi_{\text{shear}}, \quad (6)$$

where the energy ratios, R_{bulk} and R_{shear} , given in Table 2 were calculated using a finite element model programmed in COMSOL ¹.

As is shown in Figure 7, the dependence of R_{bulk} with modal frequency was a good match with the dependence of ϕ_{coating} versus frequency, indicating that the coating loss was dominated by the bulk loss. Indeed, when the data was fit there was no detectable contribution from ϕ_{shear} . The same analysis was performed on Sample 4 after the bond defects were removed by etching. The results are shown in Table 4 and Figure 6. The initial coatings yield a bulk/shear loss of $\phi_{\text{Bulk}} = (5.64 \pm 0.10) \times 10^{-4}$ and $\phi_{\text{Shear}} = (0.0 \pm 1.5) \times 10^{-6}$, while the etched coating yielded a bulk/shear loss of $\phi_{\text{Bulk}} = (5.33 \pm 0.03) \times 10^{-4}$ and $\phi_{\text{Shear}} = (0.0 \pm 5.2) \times 10^{-7}$. If we attribute the difference in the pre-etch and the post-etch ϕ_{Bulk} to the bond defects, then the bond defect loss only contributed about 5% of the total coating loss.

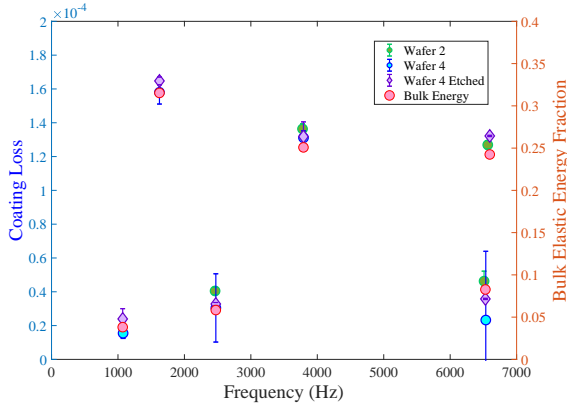


Figure 7: A comparison of variation of coating loss angle and the ratio of bulk stress energy to total stress energy versus modal frequency. The agreement illustrated the dominance of the bulk loss angle.

¹see www.comsol.com/comsol-multiphysics

To further test the validity of these results, we compared them with the coating loss calculated from the measured thermal noise of an optical cavity in Ref. [18]. Here we built a finite element model of the 35-mm long cavity and, using a spot size of 0.25 mm (beam waist radius), calculated the bulk and shear energy ratios in the AlGaAs coatings to be $R_{\text{bulk}} = 0.0898$ and $R_{\text{shear}} = 0.9102$. Using these values we predict a cavity coating loss of $\phi_{\text{coating}} = (4.78 \pm 0.05) \times 10^{-5}$, which agrees with the published result $\phi_{\text{coating}} = (4 \pm 4) \times 10^{-5}$, albeit based on measurements from a sample with an 80-fold increased coating area (or 20,000 times larger when compared with the optical spot size) than previously investigated.

5 Conclusion

Mechanical Q measurements were performed both before and after defect removal on a large-area (≈ 70 -mm diameter) substrate-transferred AlGaAs-based crystalline coating. The coating elastic loss showed a 5% reduction after defect removal, indicating that the loss contribution from the bond defects is, at most, small. A bulk/shear decomposition of the loss showed that the coating loss was due entirely to the bulk loss. The shear loss was on the order of 10^{-6} or less. This result suggests the intriguing possibility of minimizing the coating thermal noise by finding a configuration that maximizes the ratio of shear to bulk energy. With low thermal noise and excellent optical properties, GaAs/AlGaAs-based crystalline coatings are a promising candidate for future gravitational wave detectors and other precision optical applications.

Our research program will continue to investigate the source of the coating loss and methods to isolating the three loss angles for cubic crystals. On the large-area crystalline coating manufacturing front, optimization of the epitaxial growth and coating process, including the addition of post-growth polishing processes, are being investigated for the realization of defect-free crystalline coatings.

Acknowledgements

We thank Martin Fejer, Markus Aspelmeyer, and the LIGO Scientific Collaboration Optics Working group for useful discussions and feedback. This paper has been assigned LIGO Document Number ligo-p1800315.

Funding

National Science Foundation (NSF) (PHY-0107417, 1707863, 1453252, 1611821).

References

- [1] B. P. Abbott, R. Abbott, T. D. Abbott, M. R. Abernathy, and et. al Acernese. Observation of Gravitational Waves from a binary black hole merger. *Phys. Rev. Lett.*, 116:061102, Feb 2016.
- [2] B. P. Abbott, R. Abbott, T. D. Abbott, M. R. Abernathy, F. Acernese, K. Ackley, C. Adams, T. Adams, P. Addesso, R. X. Adhikari, et al. GW150914: The Advanced LIGO detectors in the era of first discoveries. *Phys. Rev. Lett.*, 116:131103, Mar 2016.
- [3] B. P. Abbott, R. Abbott, T. D. Abbott, M. R. Abernathy, and F. et al. Acernese. GW151226: Observation of Gravitational Waves from a 22-solar-mass binary black hole coalescence. *Phys. Rev. Lett.*, 116:241103, Jun 2016.
- [4] B. P. Abbott, R. Abbott, T. D. Abbott, F. Acernese, K. Ackley, C Adams, and et al. Gravitational waves and gamma-rays from a binary neutron star merger: GW170817 and GRB 170817A. *The Astrophysical Journal Letters*, 848, Oct. 2017.
- [5] Benjamin P Abbott, R Abbott, TD Abbott, MR Abernathy, F Acernese, K Ackley, C Adams, T Adams, P Addesso, RX Adhikari, et al. Prospects for observing and localizing gravitational-wave transients with Advanced LIGO, Advanced Virgo and KAGRA. *Living Reviews in Relativity*, 21(1):3, 2018.
- [6] Benjamin P Abbott, R Abbott, TD Abbott, MR Abernathy, K Ackley, C Adams, P Addesso, RX Adhikari, VB Adya, C Affeldt, et al. Exploring the sensitivity of next generation gravitational wave detectors. *Classical and Quantum Gravity*, 34(4):044001, 2017.
- [7] Matthew Abernathy, Gregory Harry, Jonathan Newport, Hannah Fair, Maya Kinley-Hanlon, Samuel Hickey, Isaac Jiffar, Andri Gretarsson, Steve Penn, Riccardo Bassiri, Eric Gustafson, Iain Martin, Sheila Rowan, and Jim Hough. Bulk and shear mechanical loss of titania-doped tantala. *Physics Letters A*, 382(33):2282 – 2288, 2018. Special Issue in memory of Professor V.B. Braginsky.
- [8] F Acernese, M Agathos, K Agatsuma, D Aisa, N Allemandou, A Allocca, J Amarni, P Astone, G Balestri, G Ballardini, et al. Advanced Virgo: a second-generation interferometric gravitational wave detector. *Classical and Quantum Gravity*, 32(2):024001, 2015.
- [9] Gregory Ashton, Eric Burns, Tito Dal Canton, Thomas Dent, H-B Eggenstein, Alex B Nielsen, Reinhard Prix, Michal Was, and Sylvia J Zhu. Coincident detection significance in multimesenger astronomy. *The Astrophysical Journal*, 860(1):6, 2018.
- [10] Yoichi Aso, Yuta Michimura, Kentaro Somiya, Masaki Ando, Osamu Miyakawa, Takatori Sekiguchi, Daisuke Tatsumi, and Hiroaki Yamamoto. Interferometer design of the kagra gravitational wave detector. *Phys. Rev. D*, 88:043007, Aug 2013.
- [11] L. Barsotti and LIGO Collaboration. The A + upgrade for Advanced LIGO. In *APS Meeting Abstracts*, page S14.002, 2018.
- [12] GariLynn Billingsley, Hiroaki Yamamoto, and Liyuan Zhang. Characterization of Advanced LIGO core optics. *Proceedings American Society for Precision Engineering (ASPE)*, 66:78–83, 2017.
- [13] H B Callen and T A Welton. Irreversibility and generalized noise. *Physical Review*, 83(1):34–40, 1951.
- [14] Tara Chalermongsak, Evan D Hall, Garrett D Cole, David Follman, Frank Seifert, Koji Arai, Eric K Gustafson, Joshua R Smith, Markus Aspelmeyer, and Rana X Adhikari. Coherent cancellation of photothermal noise in GaAs/Al 0.92Ga0.08As bragg mirrors. *Metrologia*, 53(2):860, 2016.
- [15] Garrett D Cole. Cavity optomechanics with low-noise crystalline mirrors. In *Optical Trapping and Optical Micromanipulation IX*, volume 8458, page 845807. International Society for Optics and Photonics, 2012.
- [16] Garrett D Cole, Simon Gröblacher, Katharina Gugler, Sylvain Gigan, and Markus Aspelmeyer. Monocrystalline AlxGa1-xAs heterostructures for high-reflectivity high-q micromechanical resonators in the megahertz regime. *Applied Physics Letters*, 92(26):261108, 2008.

- [17] Garrett D. Cole, Wei Zhang, Bryce J. Bjork, David Follman, Paula Heu, Christoph Deutsch, Lindsay Sonderhouse, John Robinson, Chris Franz, Alexei Alexandrovski, Mark Notcutt, Oliver H. Heckl, Jun Ye, and Markus Aspelmeyer. High-performance near- and mid-infrared crystalline coatings. *Optica*, 3(6):647–656, Jun 2016.
- [18] Garrett D Cole, Wei Zhang, Michael J Martin, Jun Ye, and Markus Aspelmeyer. Tenfold reduction of brownian noise in high-reflectivity optical coatings. *Nature Photonics*, 7(8):644, 2013.
- [19] D. Crooks, G. Cagnoli, M.M. Fejer, G. Harry, J. Hough, B.T. Khuri-Yakub, S. Penn, R. Route, S. Rowan, P.H. Sneddon, I.O. Wygant, and G.G. Yaralioglu. Experimental measurements of mechanical dissipation associated with dielectric coatings formed using SiO₂, Ta₂O₅ and Al₂O₃. *Classical and Quantum Gravity*, 23(15):4953–4965, July 2006.
- [20] A. Goldstein, P. Veres, E. Burns, M. S. Briggs, R. Hamburg, and et al. An ordinary short gamma-ray burst with extraordinary implications: Fermi-GBM detection of GRB 170817A. *The Astrophysical Journal Letters*, 848(2), 2017.
- [21] R F Greene and H B Callen. On the formalism of thermodynamic fluctuation theory. *Physical Review*, 83(6):1231–1235, 1951.
- [22] G M Harry, M R Abernathy, A E Becerra-Toledo, H Armandula, E Black, K Dooley, M Eichenfield, C Nwabugwu, A Villar, DRM Crooks, and others. Titania-doped tantala/silica coatings for gravitational-wave detection. *Classical and Quantum Gravity*, 24:405, 2007.
- [23] Gregory M Harry, LIGO Scientific Collaboration, et al. Advanced LIGO: the next generation of gravitational wave detectors. *Classical and Quantum Gravity*, 27(8):084006, 2010.
- [24] Gregory M Harry, Andri M Gretarsson, Peter R Saulson, Scott E Kittelberger, Steven D Penn, William J Startin, Sheila Rowan, Martin M Fejer, DRM Crooks, Gianpietro Cagnoli, et al. Thermal noise in interferometric gravitational wave detectors due to dielectric optical coatings. *Classical and Quantum Gravity*, 19(5):897, 2002.
- [25] M. Heurs. Gravitational wave detection using laser interferometry beyond the standard quantum limit. *Philosophical Transactions of the Royal Society of London A: Mathematical, Physical and Engineering Sciences*, 376(2120), 2018.
- [26] Ting Hong, Huan Yang, Eric K. Gustafson, Rana X. Adhikari, and Yanbei Chen. Brownian thermal noise in multilayer coated mirrors. *Phys. Rev. D*, 87:082001, Apr 2013.
- [27] Farid Khalili and Eugene S Polzik. Overcoming the SQL in gravitational wave detectors using spin systems with negative effective mass. *arXiv preprint arXiv:1710.10405*, 2017.
- [28] Maya Kinley-Hanlon, Hannah M Fair, Isaac Jiffar, Jonathan Newport, Louis Gitelman, Gregory Harry, Garilynn Billingsley, and Steve Penn. The effect of time on optical coating mechanical loss and implications for LIGO-India. *Classical and Quantum Gravity*, 33(14):147001, 2016.
- [29] Yu Levin. Internal thermal noise in the ligo test masses: A direct approach. *Physical Review D*, 57(2):659, 1998.
- [30] Manuel Marchiò, Raffaele Flaminio, Laurent Pinard, Danièle Forest, Christoph Deutsch, Paula Heu, David Follman, and Garrett D Cole. Optical performance of large-area crystalline coatings. *Optics express*, 26(5):6114–6125, 2018.
- [31] Steven D Penn, Peter H Sneddon, Helena Armandula, Joseph C Betzwieser, Gianpietro Cagnoli, Jordan Camp, D R M Crooks, Martin M Fejer, Andri M Gretarsson, Gregory M Harry, Jim Hough, Scott E Kittelberger, Michael J Mortonson, Roger Route, Sheila Rowan, and Christophoros C Vassiliou. Mechanical loss in tantala/silica dielectric mirror coatings. *Classical and Quantum Gravity*, 20(13):2917, 2003.
- [32] Stuart Reid and Iain W. Martin. Development of mirror coatings for gravitational wave detectors. *Coatings*, 6(4), 2016.
- [33] K. Ulrich Schreiber, Robert J. Thirkettle, Robert B. Hurst, David Follman, Garrett D. Cole, Markus Aspelmeyer, and Jon-Paul R. Wells. Sensing earth’s rotation with a helium neon ring laser operating at 1.15m. *Opt. Lett.*, 40(8):1705–1708, Apr 2015.
- [34] J. P. van der Ziel and M. Ilegems. Multilayer GaAs-Al_{0.3}Ga_{0.7}As dielectric quarter wave stacks grown by molecular beam epitaxy. *Appl. Opt.*, 14(11):2627–2630, Nov 1975.
- [35] Minchuan Zhou and Selim Shahriar. Broadening the sub-standard-quantum-limit region in quantum noise limited sensitivity for gravitational wave detectors. In *Frontiers in Optics*, pages FTu5A–3. Optical Society of America, 2014.